ISSN PRINT 2319 1775 Online 2320 7876

Research paper UGC CARE Listed (Group -I) Journal Volume 11, Iss 8, Dec 2022

Green Synthesis And Characterization Studies Of Calcium Doped Nickel Ferrite Nanoparticles By Microwave Combustion Method

M. Vanitha [1,2]* and G. Ramachandran [2]*

[1]Department of Chemistry, Sri Sairam Engineering College, West Tambaram, Chennai, Tamil Nadu, India.

[2]Department of Chemistry, Dr. Ambedkar Government Arts College (affiliated to University of Madras), Vyasarpadi, Chennai, Tamil Nadu, India

***Corresponding authors mail id:** vanisundar11@gmail.com (M. Vanitha); ramuvec@gmail.com (G. Ramachandran)

Abstract

Calcium doped nickel ferrite ($Ni_{1-x}Ca_xFe_2O_4$; x = 0.0, 0.1, 0.3 and 0.5) nanoparticles (NPs) were prepared by microwave irradiation technique employing the fuel L-arginine. The as prepared compositions were subjected to structural, magnetic and optical properties. Lattice constant increased with increase in calcium concentration. Transmission Electron microscope (TEM) technique provides information about morphology of the synthesized $Ni_{1-x}Ca_xFe_2O_4$ ferrites. Magnetic hysteresis (M-H) loop revealed the magnetic behavior of the prepared spinel $Ni_{1-x}Ca_xFe_2O_4$ NPs. Magnetization, coercivity and retentivity were calculated from vibrating sample magnetometer (VSM) studies. The antibacterial activity was also studied.

Keywords: $Ni_{1-x}Ca_xFe_2O_4$ ferrites; microwave irradiation; antibacterial activity; XRD.

ISSN PRINT 2319 1775 Online 2320 7876

Research paper **© 2012 IJFANS. All Rights Reserved, UGC CARE Listed (Group -I) Journal Volume 11, Iss 8, Dec 2022**

1. Introduction

Manifestation of hazardous contaminants in water bodies postures dangers for human and the environment. Activated carbon adsorption, chlorination, ultrafiltration and ozonation treatment has been used to reduce these hazardous contaminants [1-5]. Nevertheless all the above treatments are not cost effective. Hence, the preparation of ecofriendly semiconducting catalyst for the photodegradation of dyes and pollutants has attracted the attention of researchers [6-10]].

Ferrites are acknowledged for inconceivable use in the field of opto-magnetic and photoelectronic materials [11-15]. They help low energy photons to demonstrate their optical absorption and offering preferred electronic structure for its photocatalytic applications. Semiconductor spinel ferrite, with increased chemical stability generates more catalytic sites to act as a good applicant in photocatalysis [16-18]. Bacterial effluence leads to high risk for human well-being. Nanotechnology sustains an approach to improve new inorganic antimicrobial material. Hence search for nanomaterials as antibacterial agents and reviewing their properties has become an efficient research field [19-26].

A number of methods like the hydrothermal, ceramic, auto-combustion, mechanical milling, sol-gel and co-precipitation techniques are available for the preparation of ferrite nanomaterials. Amongst these the microwave irradiation method has more advantages than the other methods [28-32]. Herein, we propose calcium doped nickel ferrite ($Ni_{1-x}Ca_xFe_2O_4$; x = 0.0, 0.1, 0.3 and 0.5) NPs prepared by microwave irradiation method to study their structural, opto and magnetic properties. The as prepared nano spinel ferrites will be tested for its antibacterial activity.

ISSN PRINT 2319 1775 Online 2320 7876

Research paper **© 2012 IJFANS. All Rights Reserved, UGC CARE Listed (Group -I) Journal Volume 11, Iss 8, Dec 2022**

2. Experimental

2.1. Materials and methods

Analytical grade Iron nitrate ($Fe(NO_3)_3.9H_2O$), L-arginine ($C_6H_{14}N_4O_2$), Nickel nitrate ($Ni(NO_3)_2.6H_2O$) and Calcium nitrate ($Ca(NO_3)_2$) attained from SD fine, India, and were utilized as it is without undergoing an additional purification process.

A homogenous solution is attained by mixing precursors namely nickel nitrate and iron nitrate by maintaining a molar ratio of 1:2. It is further added to L-arginine solution, and this solution was mixed for a period of 1hr. Here, L-arginine is used as fuel and, nitrates precursor plays the role oxidizer. Oxidizer to fuel ratio was provisioned to maintain at 1, following the principle of propellant chemistry. Silica crucible was kept inside the microwave oven (SAMSUNG, India make), to which homogenous solution was poured. The microwave energy is generated by the Oven when the output power and frequency set at 900 W and 2.54 GHz respectively. Then, solution went through process namely boiling and dehydration. Consequently, vapors are produced and decomposition occurred with gas evolution. Upon achievement of spontaneous combustion by the solution, ignition occurred which results in rapid flame fluffy production of $NiFe_2O_4$. Further, the obtained samples were calcined at 550 °C for 150 min. Similarly, calcium doped samples were prepared. The samples were labeled as $NiFe_2O_4$, $Ni_{0.9}Ca_{0.1}Fe_2O_4$, $Ni_{0.7}Ca_{0.3}Fe_2O_4$ and $Ni_{0.5}Ca_{0.5}Fe_2O_4$ respectively.

The L-arginine and stoichiometry reactions of metal nitrates using in the microwave combustion process to obtain the formation of final product as follows,

$$Ni(NO_3)_2\,6H_2O_{(S)} + 2Fe(NO_3)_3\,9H_2O_{(S)} + 1.176C_6H_{14}N_4O_{2(S)} \rightarrow NiFe_2O_{4(S)} + 32.23H_2O_{(g)}\uparrow + 7.05CO_{2(g)}\uparrow + 6.35N_{2(g)}\uparrow \quad (1)$$

ISSN PRINT 2319 1775 Online 2320 7876

Research paper **© 2012 IJFANS. All Rights Reserved, UGC CARE Listed (Group -I) Journal Volume 11, Iss 8, Dec 2022**

2.2. Characterization

The as-prepared spinel $Ni_{1-x}Ca_xFe_2O_4$ (x= 0.0, 0.1, 0.3 and 0.5) NPs were analyzed by X-ray powder diffraction using Rigaku Ultima III with CuKα radiation at λ = 1.5406 Å by varying 2θ range from 20° to 80°. The morphological and elemental analysis was recorded using scanning electron microscope accompanied FEI Quanta FEG 200 with EDX analyser was employed to determine the composition of elements. The energy band gap measurement was performed using Perkin Elmer spectrophotometer. Perkin Elmer spectrophotometer is used to do FTIR studies. VSM was logged using Lake Shore, USA, Model 7404 with 3 magnets in the normal room temperature (RT).

2.3. Antibacterial activity

The antibacterial activity of spinel $NiFe_2O_4$, $Ni_{0.9}Ca_{0.1}Fe_2O_4$, $Ni_{0.7}Ca_{0.3}Fe_2O_4$ and $Ni_{0.5}Ca_{0.5}Fe_2O_4$ NPs was analyzed by their zone of inhibitions on the human pathogens gram-positive *S. aureus (Staphylococcus aureus*), *B. subtilis* (*Bacillus subtilis*) *and* gram-negative *E. coli (Escherichia coli)* and *K. pneumonia (Klebsiella pneumoniae)*. An instant culture of all microorganisms was attuned to an OD of 0.1 and wiped onto Mueller Hilton agar plates. By a cork borer, holes were stamped on the agar, followed by adding of the standard solutions containing the synthesized $NiFe_2O_4$, $Ni_{0.9}Ca_{0.1}Fe_2O_4$, $Ni_{0.7}Ca_{0.3}Fe_2O_4$ and $Ni_{0.5}Ca_{0.5}Fe_2O_4$ NPs (10µg/mL). The plates were incubated at 37˚C for 24 h and the precinct of inhibitions on the human pathogens was dignified in diameter.

3. Results and Discussion

3.1. XRD diffraction studies

ISSN PRINT 2319 1775 Online 2320 7876

Research paper **© 2012 IJFANS. All Rights Reserved, UGC CARE Listed (Group -I) Journal Volume 11, Iss 8, Dec 2022**

The structural properties of $Ni_{1-x}Ca_xFe_2O_4$ (x = 0.0, 0.1, 0.3 and 0.5) NPs were studied from the diffraction pattern obtained from XRD technique (Fig. 1). The existence of the 2θ values of 30.13˚, 35.51˚, 37.20˚, 43.23˚, 54.03˚, 57.26˚, 62.92˚ and 75.35˚ are indexed to (220), (311), (222), (400), (422), (511), (440) and (622) respectively. The lattice planes in the XRD patterns reveals the structure of single phase cubic structure with space group *Fd3m* and all the planes matched well with the JCPDS number 44-1485. The impurity peaks (*) corresponds to α-Fe_2O_3 phase verified by the card ICSD – 088418 data for $Ni_{1-x}Ca_xFe_2O_4$. The average crystallite sizes D were calculated from Scherrer formula and it ranged from 20-28 nm. The synthesized $Ni_{1-x}Ca_xFe_2O_4$ NPs are in spinel form in which Fe^{3+} ions lodge the A- site and Ni^{2+} ions the B- site [33-35]. The XRD density (XRD) was calculated by the formula:

$$dx = \frac{8M}{Na^3} = (a_x)(gm/cm^3) \quad (1)$$

where, M is molecular weight of the sample and N is Avogadro's number and 'a' is the lattice parameter. The dislocation density (δ) decreased when Ca^{2+} concentration increased upon spinel $Ni_{1-x}Ca_xFe_2O_4$ NPs ensuring the micro strain of the lattice.

Volume (V) of the prepared cubic spinel $Ni_{1-x}Ca_xFe_2O_4$ NPs were intended by using the relation,

$$v = a^3 \quad (2)$$

were V is the volume of cubic cell and a is lattice parameter of the unit cell. Values are summarized in Table 1.

W-H plot for $NiFe_2O_4$ and $Ni_{1-x}Ca_xFe_2O_4$ NPs is depicted in Fig. 2. The effective crystallite size (D) was found to be 28.48, 25.36, 23.48 and 20.58 nm respectively. Some deviation was seen in the values of (L) and (D), which was deduced using Debye Scherer's

ISSN PRINT 2319 1775 Online 2320 7876

Research paper **© 2012 IJFANS. All Rights Reserved, UGC CARE Listed (Group -I) Journal Volume 11, Iss 8, Dec 2022**

formula and W-H method respectively. It is observed that D was lower than L as there is strain factor is involved in W-H method. A positive slope was traced in Fig. 2, which confirms the presence of tensile strain [36-40]. In **Table 1** with the surging up of Ca cation content (x), an upsurge in lattice constant is seen; however, lowering in value of crystallite size was seen [27].

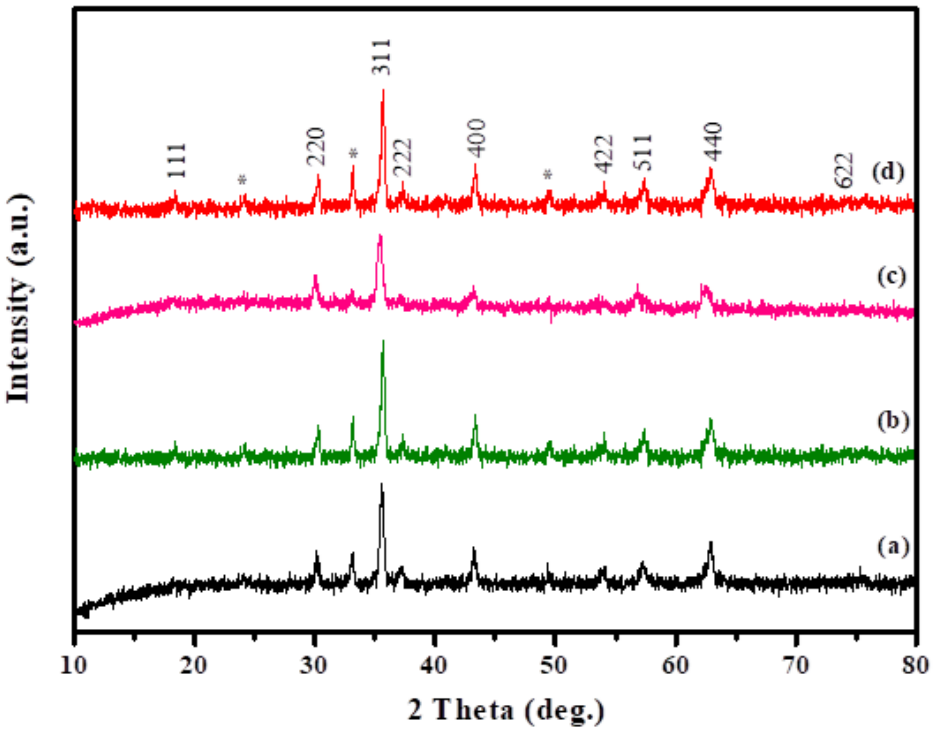

Figure 1. XRD patterns of $Ni_{1-x}Ca_xFe_2O_4$ ($0 \leq x \leq 0.5$) nanoparticles.

ISSN PRINT 2319 1775 Online 2320 7876

Research paper **© 2012 IJFANS. All Rights Reserved, UGC CARE Listed (Group -I) Journal Volume 11, Iss 8, Dec 2022**

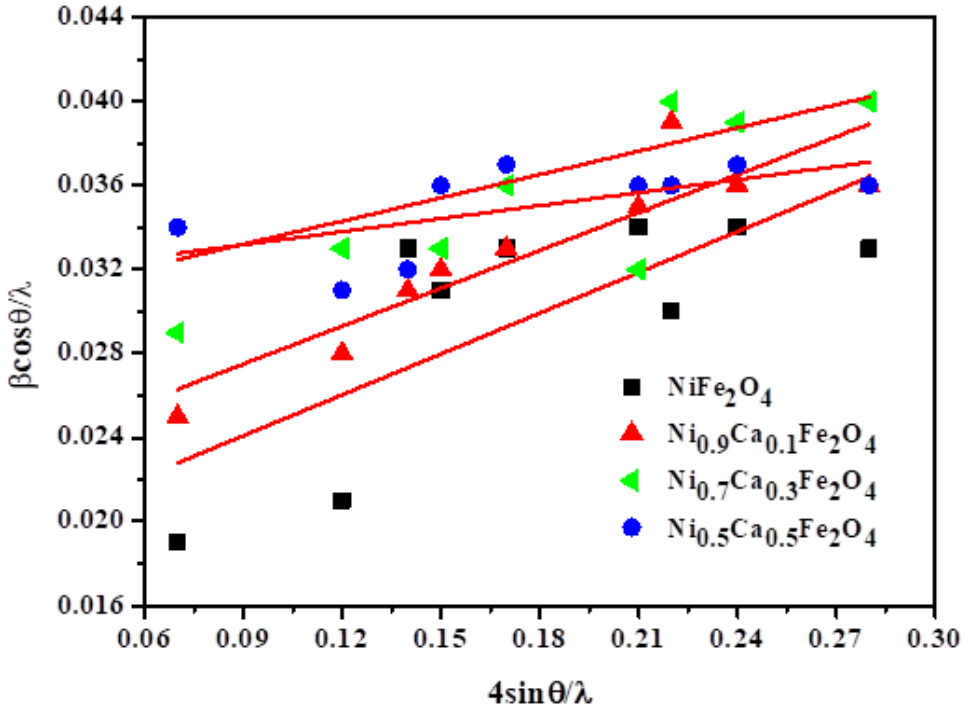

Figure 2. W-H patterns of $Ni_{1-x}Ca_xFe_2O_4$ ($0 \leq x \leq 0.5$) nanoparticles.

Table 1. Crystallite size and lattice parameter values of spinel $Ni_{1-x}Ca_xFe_2O_4$ (x= 0.0, 0.1, 0.3 and 0.5) nanoparticles.

Samples Name	Crystallite Size *L* (nm)	Effective crystallite size *D* (nm) by William-Hall plot	Lattice Parameter *a* (Å)
$NiFe_2O_4$	27.52	28.48	8.350
$Ni_{0.9}Ca_{0.1}Fe_2O_4$	25.42	25.36	8.368
$Ni_{0.7}Ca_{0.3}Fe_2O_4$	23.27	23.48	8.382
$Ni_{0.5}Ca_{0.5}Fe_2O_4$	21.76	20.58	8.396

ISSN PRINT 2319 1775 Online 2320 7876

Research paper **© 2012 IJFANS. All Rights Reserved, UGC CARE Listed (Group -I) Journal Volume 11, Iss 8, Dec 2022**

3.2. FT-IR analysis

The FT-IR spectra (Fig. 3) of $Ni_{1-x}Ca_xFe_2O_4$ (x= 0.0, 0.1, 0.3 and 0.5) NPs were studied from 400–4000 cm^{-1}. The characteristic spinel absorption band at 482 cm^{-1} and 568 cm^{-1} were accredited to the stretching vibrations, due to the interaction of oxygen and cations in Ni-O and Fe-O bond linkages [41-45]. The bands at 851 and 712 cm^{-1} are due to O-Fe-O and Fe-OH linkages and the band at 447 cm^{-1} corresponds to Fe-O linkage [46-48]. The absorption band at 642 cm^{-1} is attributed to Fe-O bond of ferrite skeleton. The broad bands at 3408 and 1626 cm^{-1} are assigned to the O-H stretching and H-O-H bending vibrations, due to the compaction of KBr pellets [49-52].

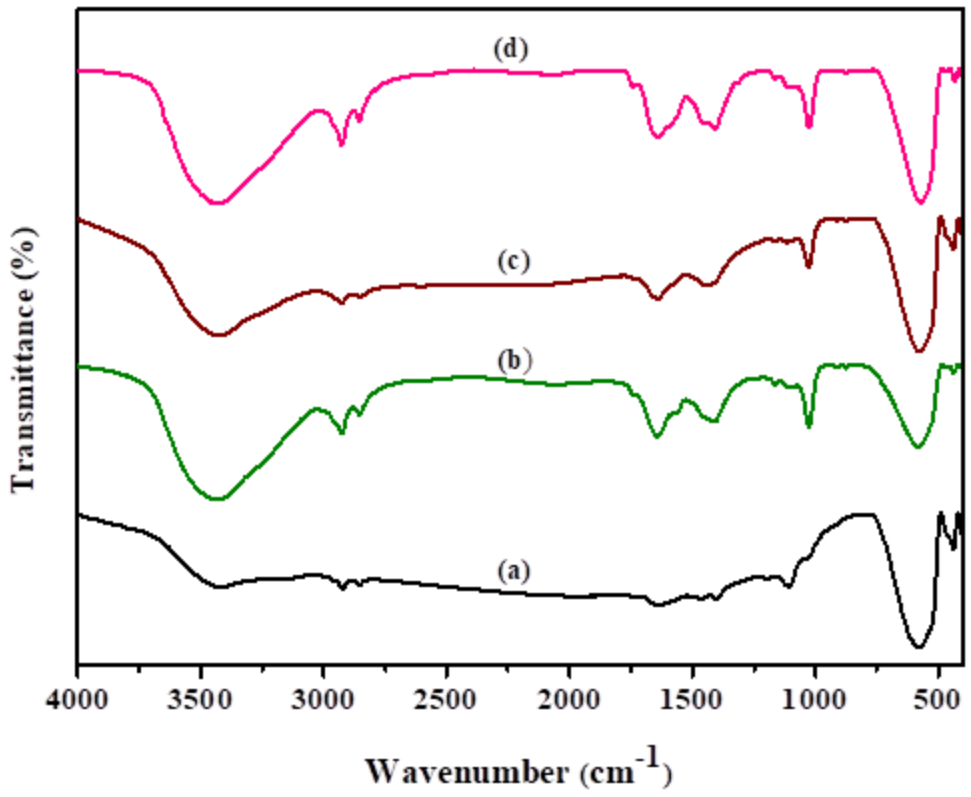

ISSN PRINT 2319 1775 Online 2320 7876

Research paper **© 2012 IJFANS. All Rights Reserved, UGC CARE Listed (Group -I) Journal Volume 11, Iss 8, Dec 2022**

Figure 3. FT-IR spectra of $Ni_{1-x}Ca_xFe_2O_4$ ($0 \leq x \leq 0.5$) nanoparticles.

3.3. HR-SEM analysis

HR-SEM images of spinel $Ni_{1-x}Ca_xFe_2O_4$ (x= 0.0, 0.1, 0.3 and 0.5) NPs revealed homogeneous spherical morphology. Further the particles exhibited coalescence and agglomerated (Fig. 4a-d), which mainly occurs due to the microwave reaction during the process of synthesis [53].

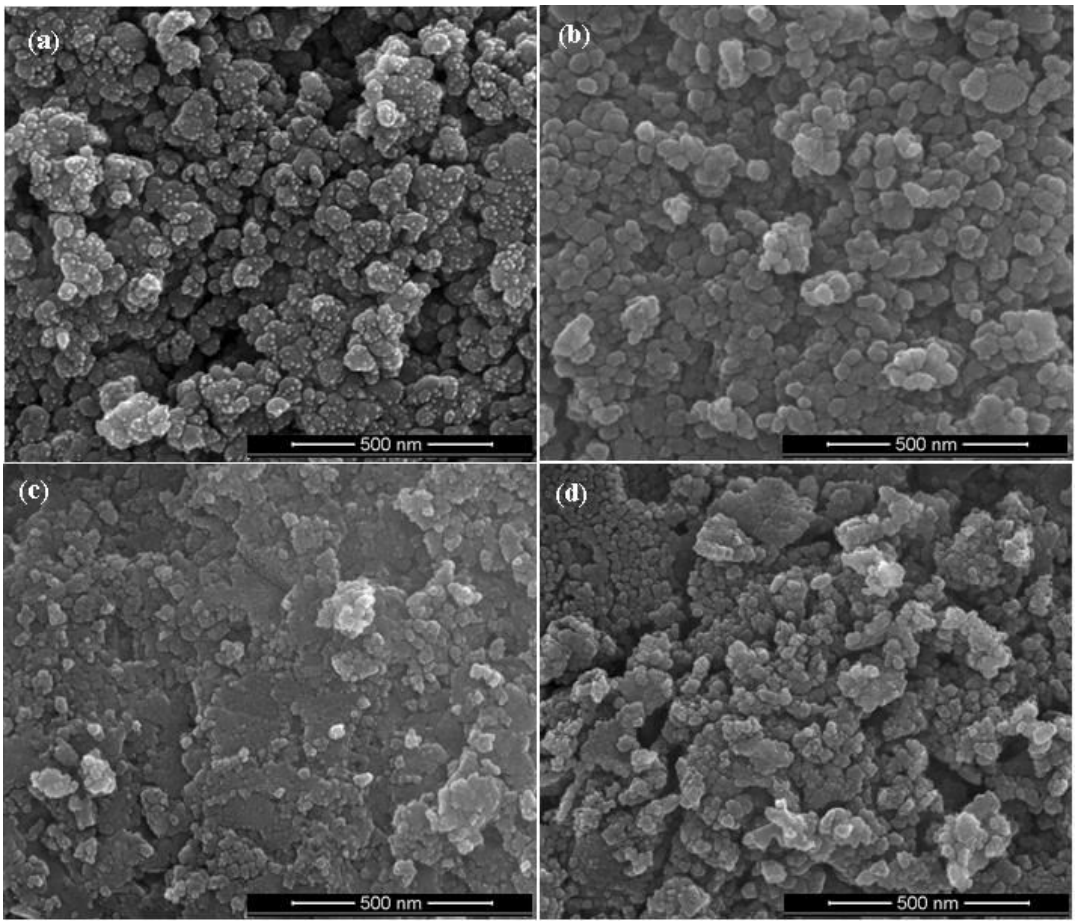

ISSN PRINT 2319 1775 Online 2320 7876

Research paper **© 2012 IJFANS. All Rights Reserved, UGC CARE Listed (Group -I) Journal Volume 11, Iss 8, Dec 2022**

Figure 4. HR-SEM images of (a) $NiFe_2O_4$, (b) $Ni_{0.9}Ca_{0.1}Fe_2O_4$, (c) $Ni_{0.7}Ca_{0.3}Fe_2O_4$ and (d) $Ni_{0.5}Ca_{0.5}Fe_2O_4$ samples.

3.4. TEM analysis

HR-TEM images (Fig.5) showed the morphology of the prepared spinel $Ni_{0.7}Ca_{0.3}Fe_2O_4$ (Fig. 5a) and $Ni_{0.5}Ca_{0.5}Fe_2O_4$ (Fig. 5b) NPs. HR-TEM images specified that the materials were crystalline in nature as the particle size ranges between 12-40 nm. The images indicate the aggregation of the material with cubical and irregular morphology of $Ni_{1-x}Ca_xFe_2O_4$ NPs [54-58]. These high diameter pictures depict the high degree of agglomerations resulting in the formation of heterogeneous surface. SAED patterns of $Ni_{0.7}Ca_{0.3}Fe_2O_4$ (Fig. 5c) and $Ni_{0.5}Ca_{0.5}Fe_2O_4$ (Fig. 5d) NPs reveal well crystalline diffraction ring and spotty ring representing the spinel structure of $Ni_{1-x}Ca_xFe_2O_4$ NPs and all the ring patterns matched with the planes obtained from XRD.

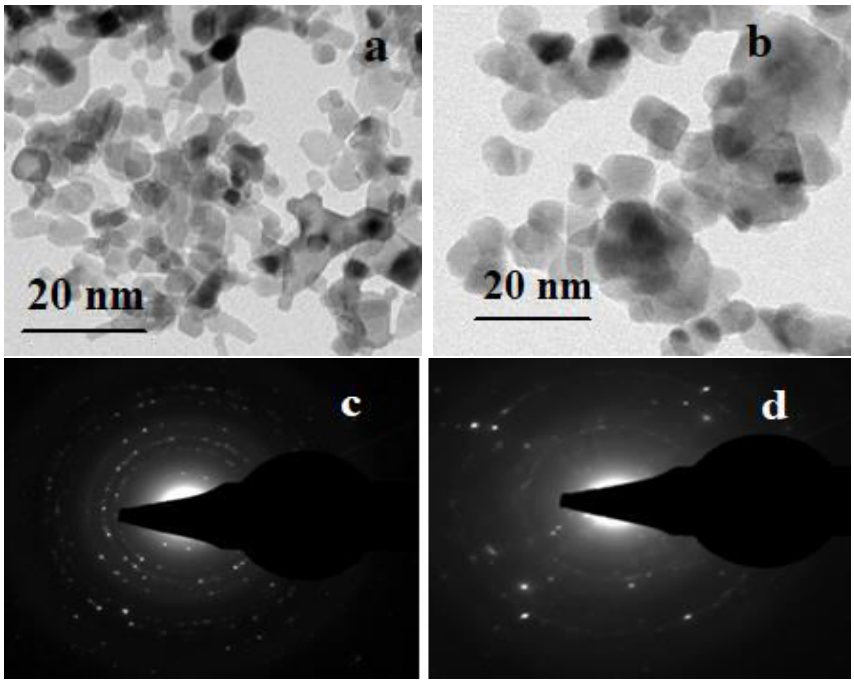

ISSN PRINT 2319 1775 Online 2320 7876

Research paper **© 2012 IJFANS. All Rights Reserved, UGC CARE Listed (Group -I) Journal Volume 11, Iss 8, Dec 2022**

Figure 5. HR-TEM images (a, b) and SAED patterns (c, d) of $Ni_{0.7}Ca_{0.3}Fe_2O_4$ and $Ni_{0.5}Ca_{0.5}Fe_2O_4$ NPs.

3.5. VSM studies

Magnetic hysteresis (M-H) curve (Fig.6) of the synthesized $Ni_{1-x}Ca_xFe_2O_4$ (x = 0.0, 0.1, 0.3 and 0.5) NPs showed weak ferromagnetic behavior, indicating that the samples are soft ferrites [59-62]. The M_s, M_r, H_c and the squareness ratio value of the M-H loops along with magnetic parameters are represented in Table 2. Lower value H_c of the synthesized spinel $Ni_{1-x}Ca_xFe_2O_4$ (x = 0.0, 0.1, 0.3 and 0.5) NPs showed the magnetically soft ferrite and distortion of spin happens on the surface due to the magneto-crystalline anisotropy.

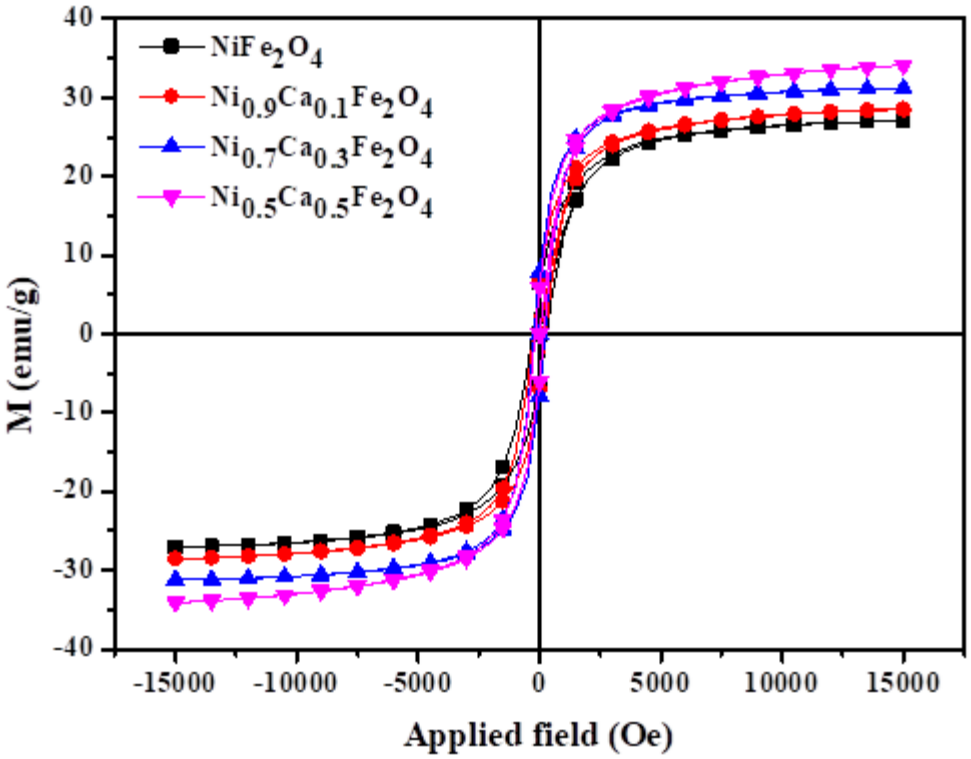

Figure 6. Magnetic hysteresis loop of $Ni_{1-x}Ca_xFe_2O_4$ ($0 \leq x \leq 0.5$) nanoparticles.

ISSN PRINT 2319 1775 Online 2320 7876

Research paper **© 2012 IJFANS. All Rights Reserved, UGC CARE Listed (Group -I) Journal Volume 11, Iss 8, Dec 2022**

Table 2. Sample name, sample code, coercivity, remanant magnetization, saturation magnetization of $Ni_{1-x}Ca_xFe_2O_4$ (x= 0.0, 0.1, 0.3 and 0.5) nanoparticles.

Samples Name	H_c, (O_e)	M_s (emu/g)	M_r (emu/g)
$NiFe_2O_4$	291.16	26.95	6.43
$Ni_{0.9}Ca_{0.1}Fe_2O_4$	285.36	24.65	6.86
$Ni_{0.7}Ca_{0.3}Fe_2O_4$	312.48	22.88	5.64
$Ni_{0.5}Ca_{0.5}Fe_2O_4$	298.55	21.63	5.98

3.6 Antibacterial study

The antibacterial activity (Fig. 7) of the synthesized spinel $Ni_{1-x}Ca_xFe_2O_4$ (x = 0.0, 0.1, 0.3 and 0.5) NPs was investigated for four bacterial pathogens comprising both gram positive and gram negative bacterial strains (Table 3). The structure and cell wall composition are different in Gram-negative and Gram-positive bacteria. The antibacterial activity varies with the bacterial pathogens [63-65]. This difference is attributed to the variation in cell wall composition and the interaction with the membrane at the cell wall or molecular level. Smaller particle size and large surface area of the synthesized spinel $Ni_{1-x}Ca_xFe_2O_4$ NPs have a tendency to interact with the cell membrane an initiate an oxidative stress thus producing an increased level of reactive oxygen species (ROS) which disrupt the bacterial cell wall. Antibacterial activity of the $Ni_{1-x}Ca_xFe_2O_4$ NPs may be attributed to chemical composition, particle size, tendency to release metal ions, penetration, and oxidation of cell components and production of ROS causing cell damage [66, 67]. In the present study the synthesised spinel $Ni_{1-x}Ca_xFe_2O_4$ NPs showed antibacterial action against both Gram-positive and Gram-negative bacteria. Fig. 7 demonstrated

ISSN PRINT 2319 1775 Online 2320 7876

Research paper **© 2012 IJFANS. All Rights Reserved, UGC CARE Listed (Group -I) Journal Volume 11, Iss 8, Dec 2022**

that the $Ni_{0.7}Ca_{0.3}Fe_2O_4$ with larger surface area showed high zone of inhibition (0-18 mm) at a concentration of 50 mg/µL against *Klebsiellapneumoniae* bacterial strain

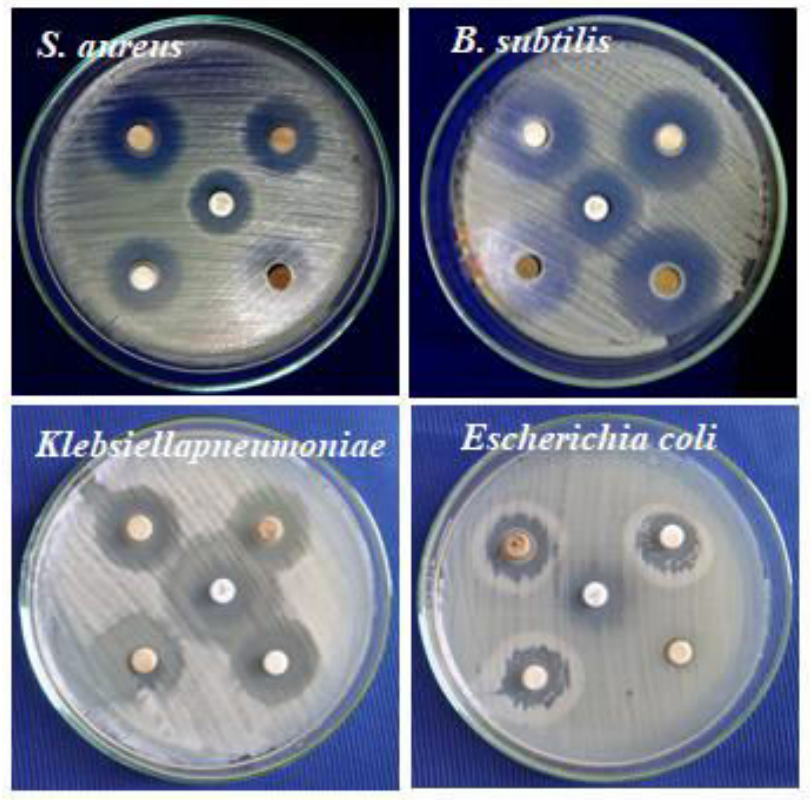

Figure 7. Antibacterial activity of $Ni_{1-x}Ca_xFe_2O_4$ ($0 \leq x \leq 0.5$) ferrite nanoparticles.

ISSN PRINT 2319 1775 Online 2320 7876

Research paper **© 2012 IJFANS. All Rights Reserved, UGC CARE Listed (Group -I) Journal Volume 11, Iss 8, Dec 2022**

Table 3. Antibacterial activity of $Ni_{1-x}Ca_xFe_2O_4$ (x = 0.0, 0.1, 0.3 and 0.5) ferrite nanoparticles.

S. No.	Bacteria	Zone of Inhibition (mm in diameter)				
		Control	x = 0.0	x = 0.1	x = 0.3	x = 0.5
1	*Bacillus subtilis*	11	13	13	13	14
2	*Staphylococcus aureus*	10	10	14	12	13
3	*Escherichia coli*	13	9	11	14	13
4	*Klebsiellapneumoniae*	15	11	12	19	16

4. Conclusions

Spinel $Ni_{1-x}Ca_xFe_2O_4$ (x = 0.0, 0.1, 0.3 and 0.5) NPs were inclined via microwave combustion technique. Powder XRD diffraction patterns revealed that spinel $Ni_{1-x}Ca_xFe_2O_4$ NPs were nano crystalline with the average crystallite size of about 12-40 nm. FT-IR spectral bands exhibited at 579, 480 and 514 cm^{-1} confirmed the stretching modes of vibration for Ni-O, Fe-O and Ca-O linkages responsible for the formation of spinel $Ni_{1-x}Ca_xFe_2O_4$ NPs. HR-TEM images displayed cubic and irregular surface morphology for the synthesized $Ni_{1-x}Ca_xFe_2O_4$ NPs. VSM analysis indicated that the as synthesized spinel $Ni_{1-x}Ca_xFe_2O_4$ were magnetically soft ferrites. Antibacterial action was tested against both Gram-positive and Gram-negative bacteria and the $Ni_{0.7}Ca_{0.3}Fe_2O_4$ showed enhanced antibacterial activity against *Klebsiellapneumoniae* associated with other compositions, due to the smaller particle size and higher surface area with the surface volume ratio of the samples.

ISSN PRINT 2319 1775 Online 2320 7876

Research paper **© 2012 IJFANS. All Rights Reserved, UGC CARE Listed (Group -I) Journal Volume 11, Iss 8, Dec 2022**

References

1. Y. Slimani, M.A. Almessiere, E. Hannachi, A. Baykal, A. Manikandan, M. Mumtaz, F. B. Azzouz, Influence of WO_3 nanowires on structural, morphological and flux pinning ability of YBa_2Cu_3Oy superconductor, Ceram. Int., 45 (2019) 2621-2628.
2. Moradmard H, Farjami Shayesteh S, Tohidi P, Abbas Z, Khaleghi M, Structural, magnetic and dielectric properties of magnesium doped nickel ferrite nanoparticles, J. Alloys.Compd.,15 (2015) 30666-6.
3. P. A. Vinosha, A. Manikandan, A. S. J. Ceicilia, A. Dinesh, G. F. Nirmala, A. Christy Preetha, Y. Slimani, M.A. Almessiere, A. Baykal, B. Xavier, Review on recent advances of zinc substituted cobalt ferrite nanoparticles: Synthesis characterization and diverse applications, Ceram. Int., 47 (2021) 10512-10535.
4. K Pamecha, V Mehta, BV Kabra, Photocatalytic Degradation of Commercial textile Azo Dye Reactive Blue 160 by Heterogeneous Photocatalysis, Adv. Appl. Sci. Res., 7 (2016) 95-101.
5. S Rajmohan, V Jeseentharani, A Manikandan, John Pragasam, Co-Precipitation Synthesis Method, Characterizations and Humidity Sensing Applications of Perovskite-Type Mixed Oxide $La_{1-x}Co_xVO_{3-\partial}$ nanocomposites, Nanosci. Nanotechnol. Lett., 8 (2016) 1-6.
6. Rimi Sharma, S Bansal, Sonal Singhal, Tailoring the photo-Fenton activity of spinel ferrites (MFe_2O_4) by incorporating different cations (M=Cu, Zn, Ni and Co) in the structure, RSC Adv., 5 (2015) 6006-6018.
7. P. Shankar, Bhavyashri, R.S. Raveendra, A. Jayasheelan, C.S. Prakash, B. Daruka Prasad, K.G. Rewathkar, B.M. Nagabhushana, Effect of temperature on electrical properties of

ISSN PRINT 2319 1775 Online 2320 7876

Research paper **© 2012 IJFANS. All Rights Reserved, UGC CARE Listed (Group -I) Journal Volume 11, Iss 8, Dec 2022**

auto combustion derived nano calcium ferrite, Int. J. Adv Sci. Tec Res, 5(5) (2016) 153-161.

8. Arunkumar Lagashetty, Amruta Pattar, Sangappa K. Ganiger, Synthesis, characterization and antibacterial study of Ag doped magnesium ferrite nanocomposite, Heliyon, 5 (2019).
9. ZZ Fang, H Wang, Densification and grain growth during sintering of nanosized particles, Int. Mater. Rev., 53 (2008) 326- 352.
10. MR Hofmann, ST Martin, WW Choi, DW Bahnemann, Environmental applications of semiconductor photocatalysis, Chem. Rev., 95 (1995) 69–96.
11. S Thiripuranthagan, D Raj, and K Kannan, Photocatalytic Degradation of Congored on Silica Supported Ag Impregnated TiO_2, J. Nanosci. Nanotech, 14 (2014) 1–7.
12. P. Thilagavathi, A. Manikandan, S. Sujatha, S. K. Jaganathan, S. Arul Antony, Sol-gel synthesis and characterization studies of $NiMoO_4$ nanostructures for photocatalytic degradation of methylene blue dye, Nanosci. Nanotech. Lett., 8 (2016) 438-443.
13. K. Seevakan, A. Manikandan, P. Devendran, Y. Slimani, A. Baykal, T.Alagesan, Structural, morphological and magneto-optical properties of $CuMoO_4$ electrochemical nanocatalyst as supercapacitor electrode, Ceramics International, 44 (2018) 20075-20083
14. Bamzai K. K, Gurbinder Kour, Balwinder Kaur, Kulkarni S. D, Preparation, and Structural and Magnetic Properties of Ca Substituted Magnesium Ferrite with Composition $MgCa_xFe_{2-x}O_4$ (x = 0.00, 0.01, 0.03, 0.05, 0.07) Journal of Materials., (2014), 8.
15. Mahboubeb Houshiau, Fatemeh Zebhi, Zahra Jafari Razi, Ali Alidoust, Zohuh Askari, Synthesis of cobalt ferrite nanoparticles using combustion, coprecipiation, and

ISSN PRINT 2319 1775 Online 2320 7876

Research paper **© 2012 IJFANS. All Rights Reserved, UGC CARE Listed (Group -I) Journal Volume 11, Iss 8, Dec 2022**

precipitation methods: A comparison of structural, size and magnetic properties, J.Magn. Magn.Mater, 371 (2014) 43-48.

16. AK Nikumbh, , RA Pawar, DV Nighot, GS Gugale, MD Sangale, MB Khanvilkar, AV Nagawade, Structural, electrical, magnetic and dielectric properties of rare-earth substituted cobalt ferrites nanoparticles synthesized by the co-precipitation method, J.Magn. Magn.Mater, 355 (2014) 201-209.
17. V. Muthuvignesh, S. K. Jaganathan, A. Manikandan, Nanomaterials as a game changer in the management and treatment of diabetic foot ulcers, RSC Adv., 6 (2016) 114859-114878.
18. V. Muthuvignesh, V.J. Reddy, S. Ramakrishna, S. Ray, A. Ismail, M. Mandal, A. Manikandan, S. Seal and S. K. Jaganathan, Electrospinning applications from diagnosis to treatment of diabetes, RSC Adv., 6 (2016) 83638-83655.
19. R. R. Mathiarasu, A. Manikandan, K. Panneerselvam, M. George, Y. Slimani, M. A. Almessiere, A. Baykal, A. M. Asiri, T. Kamal, A. Khan, Photocatalytic degradation of reactive anionic dyes RB5, RR198 and RY145 via Rare earth element (REE) Lanthanum substituted $CaTiO_3$ perovskite catalysts, J. Mater. Res. Tech., 15 (2021) 5936-5947.
20. M. A. Almessiere, Y. Slimani, N. A. Algarou, M. A. Gondal, Y. S. Wudil, M. Younas, I. A. Auwal, A. Baykal, A. Manikandan, Investigation on electrical and dielectric properties of hard/soft spinel ferrite nanocomposites of $CoFe_2O_4/(NiSc_{0.03}Fe_{1.97}O_4)x$, Vacuum, 194 (2021) 110628.
21. M. A. Almessiere, Y. Slimani, N. A. Algarou, M. A. Gondal, Y. S. Wudil, M. Younas, I. A. Auwal, A. Baykal, A. Manikandan, Electrospinning synthesis of Cd substituted Ni-Co

ISSN PRINT 2319 1775 Online 2320 7876

Research paper **© 2012 IJFANS. All Rights Reserved, UGC CARE Listed (Group -I) Journal Volume 11, Iss 8, Dec 2022**

spinel ferrite nanofibers: An investigation on their structural and magnetic features, Appl. Phys. A, 127 (2021) 785.

22. A. Alagarsamy, S. Chandrasekaran, A. Manikandan, Green synthesis and characterization studies of biogenic zirconium oxide (ZrO_2) nanoparticles for adsorptive removal of methylene blue dye, J. Mol. Struct., 1247 (2022) 131275.
23. M.A. Almessiere, S. Güner, Y. Slimani, A. Baykal, Sagar E. Shirsath, A. Demir Korkmaz, R. Badar, A. Manikanadan, Investigation on the structural, optical, and magnetic features of Dy^{3+} and Y^{3+} co-doped $Mn_{0.5}Zn_{0.5}Fe_2O_4$ nanospinel ferrite nanoparticles, J. Mol. Struct., 1248 (2022) 131412.
24. M. A. Almessiere, Y. Slimani, Y. O. Ibrahim, M. A. Gondal, M. A. Dastageer, I. A. Auwal, A. V. Trukhanov, A. Manikandan, A. Baykal, Morphological, structural, and magnetic characterizations of hard-soft ferrite nanocomposites synthesized via pulsed laser ablation in liquid, Mater. Sci. Eng. B, 273 (2021) 115446
25. M. A. Almessiere, Y. Slimani, N. A. Algarou, M. A. Gondal, Y. S. Wudil, M. Younas, I. A. Auwal, A. Baykal, A. Manikandan, T. I. Zubar, V. G. Kostishin, A. V. Trukhanov, I. Ercan, Electronic, magnetic, and microwave properties of hard/soft nanocomposites based on hexaferrite $SrNi_{0.02}Zr_{0.02}Fe_{11.96}O_{19}$ with variable spinel phase MFe_2O_4 (M = Mn, Co, Cu, and Zn), Ceram. Int., 47 (2021) 35209-35223.
26. M.A. Almessiere, B. Unal, Y. Slimani, H. Gungunes, M.S. Toprak, N. Tashkand, A. Baykal, M. Sertkol, A.V. Trukhanov, A. Yıldız, A. Manikandan, Effects of Ce-Dy rare earths co-doping on various features of Ni-Co spinel ferrite microspheres prepared via hydrothermal approach, J. Mater. Res. Technol., 14 (2021) 2534-2553.

ISSN PRINT 2319 1775 Online 2320 7876

 UGC CARE Listed (Group -I) Journal Volume 11, Iss 8, Dec 2022

27. V. S. P. Sakthi Sri, A. Manikandan, M. Mathankumar, R. Tamizhselvi, M. George, A. L. Bilgrami, S. A. Al-Zahrani, A. A. P. Khan, Anish Khan, A. M. Asiri, Unveiling the photosensitive, mechanical and magnetic properties of amorphous iron nanoparticles with its application towards decontamination of water and cancer treatment, J. Mater. Res. Technol., 15 (2021) 99-118.

28. K. Geetha, R. Udhayakumar, A. Manikandan, Enhanced magnetic and photocatalytic characteristics of cerium substituted spinel $MgFe_2O_4$ ferrite nanoparticles, Physica B, 615 (2021) 413083.

29. S. S. Al-Jameel, S. Rehman, M. A. Almessiere, F. A. Khan, Y. Slimani, N. S. Al-Saleh, A. Manikandan, E. A. Al-Suhaimi, A. Baykal, Anti-microbial and anti-cancer activities of $MnZnDy_xFe_{2-x}O_4$ ($x \leq 0.1$) nanoparticles, Artificial Cells, Nanomedicine and Biotechnology, 49 (2021) 493-499.

30. S. Rehman, M. A. Almessiere, S. S. Al-Jameel, U. Ali, Y. Slimani, N. Taskhandi, N. S. Al-Saleh, A. Manikandan, F. A. Khan, E. A. Al-Suhaimi, A. Baykal, Designing of $Co_{0.5}Ni_{0.5}Ga_xFe_{2-x}O_4$ ($0.0 \leq x \leq 1.0$) Microspheres via Hydrothermal Approach and Their Selective Inhibition on the Growth of Cancerous and Fungal Cells, Pharmaceutics, 13 (2021) 962.

31. A. Muthukrishnaraj , S. A. Al-Zahrani , A. Al Otaibi , S. S. Kalaivani, A. Manikandan, N. Balasubramanian, A. L. Bilgrami, M. A. R. Ahamed, A. Khan, A. M. Asiri, N. Balasubramanian, Enhanced Photocatalytic Activity of Cu_2O Cabbage/RGO Nanocomposites under Visible Light Irradiation, Polymers, 13 (2021) 1712.

ISSN PRINT 2319 1775 Online 2320 7876

Research paper **© 2012 IJFANS. All Rights Reserved, UGC CARE Listed (Group -I) Journal Volume 11, Iss 8, Dec 2022**

32. M. A. Almessiere, B. Unal, I.A. Auwal, Y. Slimani, H. Aydin, A. Manikandan, A. Baykal, Impact of calcination temperature on electrical and dielectric properties of $SrGa_{0.05}Fe_{11.98}O_4$-$Zn_{0.5}Ni_{0.5}Fe_2O_4$ hard/soft nanocomposites, J. Mater. Sci. Mater. Electron., 32 (2021) 16589-16600.

33. O. Alagha, N. Ouerfelli, H. Kochkar, M. A. Almessiere , Y. Slimani, A. Manikandan, A. Baykal, A. Mostafa, M. Zubair, M. H. Barghouthi, Kinetic Modeling for Photo-Assisted Penicillin G Degradation of $(Mn_{0.5}Zn_{0.5})[Cd_xFe_{2-x}]O_4$ ($x \leq 0.05$) Nanospinel Ferrites, Nanomaterials, 11 (2021) 970.

34. M. R. Ranjitha, A. Manikandan, J. N. Baby, K. Panneerselvam, S. Ragu, Mary George, Y. Slimani, M.A. Almessiere, A. Baykal, Hexagonal basalt-like ceramics $La_xMg_{1-x}TiO_3$ (x = 0 and 0.5) contrived via deep eutectic solvent for selective electrochemical detection of dopamine, Physica B, 615 (2021) 413068.

35. P. Annie Vinosha, A. Manikandan, A. Christy Preetha, A. Dinesh, Y. Slimani, M.A. Almessiere, A. Baykal, Belina Xavier, G. Francisco Nirmala, Review on recent advances of synthesis, magnetic properties and water treatment applications of cobalt ferrite nanoparticles and nanocomposites, J. Supercond. Nov. Magn., 34 (2021) 995–1018.

36. M. A. Almessiere, Y. Slimani, H. Güngüneş, K. A. Demir, Z. Tatiana, T. Sergei, T. Alex, A. Manikandan, A. Fatimah, A. Baykal, Influence of Dy^{3+} ions on microstructure, magnetic, electrical and microwave properties of $[Ni_{0.4}Cu_{0.2}Zn_{0.4}](Fe_{2-x}Dy_x)O_4$ ($0.00<x<0.04$) spinel ferrites, ACS Omega, 6 (2021) 10266-10280.

37. S. S. Al-Jameel, M. A. Almessiere, F. A. Khan, N. Taskhandi , Y. Slimani, N. S. Al-Saleh, A. Manikandan, E. A. Al-Suhaimi, A. Baykal, Synthesis, Characterization, Anti-Cancer

ISSN PRINT 2319 1775 Online 2320 7876

 UGC CARE Listed (Group -I) Journal Volume 11, Iss 8, Dec 2022

Analysis of $Sr_{0.5}Ba_{0.5}Dy_xSm_xFe_{8-2x}O_{19}$ ($0.00 \leq x \leq 1.0$) Microsphere Nanocomposites, Nanomaterials, 11 (2021) 700.

38. Y. Slimani, N. A. Algarou, M. A. Almessiere, A. Sadaqat M. G. Vakhitov, D. S. Klygach, D. I. Tishkevich, A. V. Trukhanov, S. Güner, A. S. Hakeem, I. A. Auwal, A. Baykal, A. Manikandan, I. Ercan, Fabrication of exchanged coupled hard/soft magnetic nanocomposites: Correlation between composition, magnetic, optical and microwave properties, Arabian J. Chem., 10 (2021) 102992.
39. P. A. Vinosha, A. Manikandan, A. S. J. Ceicilia, A. Dinesh, G. F. Nirmala, A. Christy Preetha, Y. Slimani, M.A. Almessiere, A. Baykal, B. Xavier, Review on recent advances of zinc substituted cobalt ferrite nanoparticles: Synthesis characterization and diverse applications, Ceram. Int., 47 (2021) 10512-10535.
40. M. A. Almessiere, Y. Slimani, İ. A. Auwal, S. E. Shirsath, A. Manikandan, A. Baykal, B. Özçelik, I. Ercan, Sergei V. Trukhanov, Denis A. Vinnik, Alex V. Trukhanov, Impact of Tm^{3+} and Tb^{3+} Rare Earth Cations Substitution on the Structure and Magnetic Parameters of Co-Ni Nanospinel Ferrite, Nanomaterials, 10 (2020) 2384.
41. N. A Algarou, Y. Slimani, M. A. Almessiere, A. Sadaqat, A. V. Trukhanov, M. A. Gondal, A. S. Hakeem, S. V. Trukhanov, M. G. Vakhitov, D. S. Klygach, A. Manikandan, A. Baykal, Functional $Sr_{0.5}Ba_{0.5}Sm_{0.02}Fe_{11.98}O_4/x(Ni_{0.8}Zn_{0.2}Fe_2O_4)$ Hard–Soft Ferrite Nanocomposites: Structure, Magnetic and Microwave Properties, Nanomaterials, 10 (2020) 2134.
42. P. Annie Vinosha, A. Manikandan, R. Ragu, A. Dinesh, P. Paulraj, Y. Slimani, M.A. Almessiere, A. Baykal, J. Madhavan, B. Xavier, G. Francisco Nirmala, Exploring the

ISSN PRINT 2319 1775 Online 2320 7876

Research paper **© 2012 IJFANS. All Rights Reserved, UGC CARE Listed (Group -I) Journal Volume 11, Iss 8, Dec 2022**

influence of varying pH on structural, electro-optical, magnetic and photo-Fenton properties of mesoporous $ZnFe_2O_4$ nanocrystals, Environmental Pollution, 272 (2021) 115983.

43. P. Annie Vinosha, A. Manikandan, R. Ragu, Y. Slimani, A. Baykal, Belina Xavier, Impact of nickel substitution on structure, magneto-optical, electrical and acoustical properties of cobalt ferrite nanoparticles, J. Alloys Compd., 857 (2021) 157517.
44. T. L. Ajeesha, A. Ashwini, Mary George, A. Manikandan, J. Arul Mary, Y. Slimani, M. A. Almessiere, A. Baykal, Nickel substituted $MgFe_2O_4$ nanoparticles via co-precipitation method for photocatalytic applications, Physica B: 606 (2021) 412660.
45. A. Manikandan, M. Yogasundari, A. Dinesh, K. Thanrasu, K. Kanmani Raja, Y. Slimani, S. K. Jaganathan, A. Baykal, Synthesis and characterizations of multifunctional magnetic-luminescent $ZnO@Fe_3O_4$ nanocomposites, Physica E, 124 (2020) 114291.
46. S. Rathinavel, R. Deepika, D. Panda, A. Manikandan, Synthesis and characterization of $MgFe_2O_4$ and $MgFe_2O_4$/rGO nanocomposites for the photocatalytic degradation of methylene blue, Inorganic and Nano-Metal Chemistry, 51, 2 (2021) 210-217.
47. M A Almessiere, Y Slimani, H Gungunes, M Nawaz, F S Al-ahmari, A Manikandan, A Baykal, Investigation of the crystal/magnetic structure, magnetic and optical properties of $SrY_xNb_xFe_{12-2x}O_{19}$ ($x \leq 0.05$) hexaferrites, Physica Scripta, 95 (2020) 055802
48. R. A. Senthil, S. Osman, J. Pan, A. Khan, V. Yang, T. R. Kumar, Y. Sun, A. Manikandan, One-pot preparation of AgBr/α-Ag_2WO_4 composites with superior

ISSN PRINT 2319 1775 Online 2320 7876

Research paper **© 2012 IJFANS. All Rights Reserved, UGC CARE Listed (Group -I) Journal Volume 11, Iss 8, Dec 2022**

photocatalytic activity under visible-light irradiation, Colloids and Surfaces A: Physicochemical and Engineering Aspects, 586 (2020) 124079.

49. M. A. Almessiere, Y. Slimani, A. Demir Korkmaz, A. Baykal, H. Gungunes, H. Sozeri, Sagar E. Shirsath, S. Guner, S. Akhtar, A. Manikandan, Impact of La^{3+} and Y^{3+} ion substitutions on structural, magnetic and microwave properties of $Ni_{0.3}Cu_{0.3}Zn_{0.4}Fe_2O_4$ nanospinel ferrites synthesized via sonochemical route, RSC Adv., 9 (2019) 30671–30684.
50. Y. Slimani, M. A. Almessiere, A. D. Korkmaz, H. Güngüneş, M.Sertkol, A. Manikandan, A. Yildiz, S. Akhtar, Sagar E. Shirsath, $Ni_{0.4}Cu_{0.2}Zn_{0.4}Tb_xFe_{2-x}O_4$ nanospinel ferrites: Ultrasonic synthesis and physical properties, Ultrasonics Sonochemistry, 59 (2019) 104757.
51. M. A. Almessiere, Y. Slimani, H. Güngüneş, S. Ali, A. Manikandan, I. Ercan, A. Baykal, A.V. Trukhanov, Magnetic Attributes of $NiFe_2O_4$ Nanoparticles: Influence of Dysprosium Ions (Dy^{3+}) Substitution, Nanomaterials, 9 (2019) 280.
52. R. A. Senthil, S. Osman, J. Pan, Y. Sun, T. R. Kumar, A. Manikandan, A facile hydrothermal synthesis of visible-light responsive $BiFeWO_6/MoS_2$ composite as superior photocatalyst for degradation of organic pollutants, Ceram. Int., 45 (2019) 18683-18690.
53. M. A. Almessiere, Y. Slimani, H. Gungunes, A. Manikandan, A. Baykal, Investigation of the effects of Tm^{3+} on the structural, microstructural, optical, and magnetic properties of Sr hexaferrites, Results in Physics, 13, (2019) 102166.
54. A.D. Korkmaz, S. Güner; Y. Slimani, H. Gungunes, Md. Amir; A. Manikandan, A. Baykal, Microstructural, optical and magnetic properties of vanadium substituted nickel spinel nano-ferrites, J. Supercond. Nov. Magn., 32 (2019) 1057–1065.

ISSN PRINT 2319 1775 Online 2320 7876

Research paper **© 2012 IJFANS. All Rights Reserved, UGC CARE Listed (Group -I) Journal Volume 11, Iss 8, Dec 2022**

55. Y. Slimani, A. Baykal, Md. Amir, N. Tashkandi, H. Güngüneş, S. Guner, H.S. El Sayed, F. Aldakheel, T.A. Saleh, A. Manikandan, Substitution effect of Cr^{3+} on hyperfine interactions, magnetic and optical properties of Sr-hexaferrites, Ceram. Int., 44 (2018) 15995-16004.

56. A. Baykal, S. Guner, H. Gungunes, K.M. Batoo, Md. Amir, A. Manikandan, Magneto Optical Properties and hyperfine interactions of Cr^{3+} ion substituted copper ferrite nanoparticles, J. Inorg. Organomet. Polym., 28 (2018) 2533–2544.

57. Y. Slimani, H. Gungunes, M. Nawaz, A. Manikandan, H.S. El Sayed, M.A. Almessiere, H. Sozeri, S.E. Shirsath, I. Ercan, A. Baykal, Magneto-optical and microstructural properties of spinel cubic copper ferrites with Li-Al co-substitution, Ceram. Int., 44 (2018) 14242-14250.

58. Md Amir, H. Gungunes, Y. Slimani, N. Tashkandi, H.S. El Sayed, F. Aldakheel, M. Sertkol, H. Sozeri, A. Manikandan, I. Ercan, A. Baykal, Mossbauer studies and magnetic properties of cubic $CuFe_2O_4$ nanoparticles, J. Supercond. Nov. Magn., 32 (2018) 557–564

59. P. Bhavani, A. Manikandan, S. K. Jaganathan, S. Shankar, S. Arul Antony, Enhanced catalytic activity, facile synthesis and characterization studies of spinel Mn-Co aluminate nano-catalysts, J. Nanosci. Nanotech., 18 (2018) 1388–1395.

60. Md Amir, H. Gungunes, A. Baykal, M. Almessiere, H. Sozeri, I. Ercan, M. Sertkol, S. Asiri, A Manikandan, Effect of annealing temperature on Magnetic and Mossbauer properties of $ZnFe_2O_4$ nanoparticles by sol-gel approach, J. Supercond. Nov. Magn., 31 (2018) 3347–3356.

ISSN PRINT 2319 1775 Online 2320 7876

 UGC CARE Listed (Group -I) Journal Volume 11, Iss 8, Dec 2022

61. S. Asiri, S. Güner, A. Demir, A. Yildiz, A. Manikandan, A. Baykal, Synthesis and Magnetic Characterization of Cu Substituted Barium Hexaferrites, J. Inorg. Organomet. Polym., 28 (2018) 1065–1071.

62. S. Asiri, M. Sertkol, S. Guner, H. Gungunes, K.M. Batoo, T.A. Saleh, H. Sozeri, M.A. Almessiere, A. Manikandan, A. Baykal, Hydrothermal synthesis of $Co_yZn_yMn_{1-2y}Fe_2O_4$ nanoferrites: Magneto-optical investigation, Ceram. Int., 44 (2018) 5751–5759.

63. A. Godlyn Abraham, A. Manikandan, E. Manikandan, S. Vadivel, S. K. Jaganathan, A. Baykal, P. Sri Renganathan, Enhanced magneto-optical and photo-catalytic properties of transition metal cobalt (Co^{2+} ions) doped spinel $MgFe_2O_4$ ferrite nanocomposites, J. Magn. Magn. Mater., 452 (2018) 380-388.

64. R. Bomila, S. Srinivasan, S. Gunasekaran, A. Manikandan, Enhanced photocatalytic degradation of methylene blue dye, opto-magnetic and antibacterial behaviour of pure and La-doped ZnO nanoparticles, J. Supercond. Nov. Magn., 31 (2018) 855–864.

65. K. Elayakumar, A. Dinesh, A. Manikandan, P. Murugesan, G. Kavitha, S. Prakash, R. T. Kumar, S. K. Jaganathan, A. Baykal, Structural, morphological, enhanced magnetic properties and antibacterial bio-medical activity of rare earth element (REE) Cerium (Ce^{3+}) doped $CoFe_2O_4$ nanoparticles, J. Magn. Magn. Mater., 476 (2019) 157-165.

66. A.T. Ravichandran, J. Srinivas, A. Manikandan, A. Baykal, Enhanced magneto-optical and antibacterial studies of $Bi_{1-x}Mg_xFeO_3$ ($0.0 \leq x \leq 0.15$)) nanoparticles, J. Supercond. Nov. Magn., 32 (2019) 1663–1670.

67. M. George, T.L. Ajeesha, A. Manikandan, Ashwini Anantharaman, R.S. Jansi, E. Ranjith Kumar, Y. Slimani, M.A. Almessiere, A. Baykal, Evaluation of Cu-$MgFe_2O_4$

ISSN PRINT 2319 1775 Online 2320 7876

 UGC CARE Listed (Group -I) Journal Volume 11, Iss 8, Dec 2022

spinel nanoparticles for photocatalytic and antimicrobial activates, J. Phys. Chem. Solids, 153 (2021) 110010.